Testing coalescence and statistical-thermal production scenarios for (anti-)(hyper-)nuclei at LHC energies with recent and future Run 3 and 4 data

F. Bellini and A. Kalweit

26th of February 2018

(Anti-)(hyper-)nuclei are unique probes of the medium created in proton-proton, proton-Pb, and Pb–Pb collisions at LHC energies. At LHC energies, their production is typically discussed within the framework of coalescence and thermal-statistical production models. While it is often argued that both approaches are not distinguishable, we present a detailed study of both theories which reveals largely different predictions between the two approach for the production of 3He and hyper-tritons. Confronting our results with recent ALICE measurements, the coalescence approach is found to provide a correct description of the data only in small systems such as pp collisions, while it fails for central Pb–Pb collisions. The thermal-statistical model on the other hand is in agreement with results in central Pb–Pb collisions even though such fragile objects should be destroyed in hadronic interactions after the chemical freeze-out of the system. Our finding thus indicate the existence of a novel production mechanism for these objects.

Contents

1 Introduction

The formation of light anti- and hyper- nuclei in highly energetic proton-proton, proton-nucleus and nucleus-nucleus collisions provides unique observables for the study of the system created in these collisions. In this context, nuclei and hyper-nuclei are special objects with respect to non-composite hadrons, because their size is comparable to a fraction or the whole system created in the collision []. The relevant properties of the objects under study are summarised in Table 1 As quantum-mechanical objects, their size is typically defined as the rms of their wave function, which ranges from xx fm for the 3He up to yy fm for the hyper-triton. Halo nuclei as 6He would be ideal for such studies, but they remain out of the experimental reach in high-energy experiments in the near future.

Surprisingly, thermal-statistical models have been successful at describing not only light-flavour particle production, but also that of light (anti-)(hyper-)nuclei across a wide range of energies in nucleus-nucleus collisions [**?**, **?**]. In this approach, particles are produced from a fireball in thermal and kinetic equilibrium with temperatures of the order of $T_{chem} = 156$ MeV (near the temperature at the QCD phase transition boundary, as predicted by lattice QCD calculations [**?**]. Particle abundances are fixed at chemical freeze-out, when inelastic collisions cease. Further elastic and pseudo-elastic collisions occur among the components of the expanding fireball, that can affect the spectral shapes and the measurable yields of short-lived (strongly decaying) hadronic resonances. Once the particle density of the system is so low that the mean free path for elastic collisions is larger than the size of the system, the fireball freezes-out kinetically. This is seen to occur when the system has reached temperatures of the order of $T_{kin} \approx 90$ MeV. In such a dense and hot environment, composite objects with binding energies that are small with respect to the temperature of the system, appear as "fragile" objects. For instance, the binding energy of the deuteron is $E_{B,d} = 2.2$ MeV $\ll T_{chem}, T_{kin}$. As a matter of fact, the cross-section for pion-induced deuteron breakup is significantly larger than the typical (pseudo)-elastic cross-sections for the re-scattering of hadronic resonance decay products (check statement and refer to Juergen's QM proceedings) [**?**, **?**]. Similarly, the elastic cross-section which drives the deuteron spectra to kinetic equilibration in central heavy-ion collisions [**?**] is smaller than the breakup cross-section [**?**]. Based on this, the deuterons produced at chemical freeze-out would be expected not to survive the hadronic phase of the medium expansion, yet their production is measured to be consistent to the predictions from statistical-thermal models and they develop also a non-zero elliptic flow which is consistent with a common radial expansion together with the non-composite hadrons [**?**]. Do similar estimates as Karel in Frascati. In addition, it was recently shown that the assumption of realistic eigenvolumina for light nuclei would lead to instabilities of the statistical/thermal model predictions [**?**]. Several solutions have been proposed to solve this "light (anti-)nuclei puzzle": (a.) a sudden freeze-out at the QGP-hadron phase boundary, (b.) the thermal production of these objects as compact quark bags [**?**], and (c.) the coincidence of coalescence mechanism with that of thermal production [**?**]. Data from rescattering of short-lived hadronic resonances indicate that the system undergoes a long-lasting hadronic phase before decoupling [], thus strongly disfavouring hypothesis (a.). While hypothesis (b.) cannot presently be tested beyond the agreement of measured (anti-)nuclei production yields with statistical-thermal model predictions, hypothesis (c.) is scrutinised in the present work.

To this purpose, we compare to models the existing data from the Large Hadron Collider. For the first time, these data allow for the systematic study of the light (anti-)(hyper-)nuclei production as a function of the system and object size. In the nucleon-coalescence approach, nuclei are formed at kinetic freeze-out by coalescence of nucleons that are nearby in space and have similar velocities. The coalescence model is reviewed in Section 2, starting from its simplest form (uncorrelated nucleon emission from a point-like source) to the full space-time evolution picture as discussed in [**?**]. In section 3, a blast-wave parameterisation for particle transverse momentum spectra in combination with predictions from the statistical-thermal model for the yields is used as an alternative approach. The direct comparison of the two approaches and the comparison with data are discussed in section 4. We find that a systematic study of the coalescence parameter B_A provides an important discrimination power between the two approaches. In section 5 we propose that B_A is systematically measured in all collision systems by exploiting the large statistics sample that will be available with the LHC Run 3 and 4, in order to rule out or support the aforementioned scenarios. As a matter of fact, the upcoming years of LHC data taking provide a unique opportunity to for the final understanding of (anti-)(hyper-

)nuclei production. Setting a final word on the production mechanisms is not only in the interest of the heavy-ion community, but has a broader application in astrophysics and dark-matter searches, by representing an essential input for the measurement of (anti-)nuclei in space with ongoing [?] and future [?, ?] experiments. In addition to this, the study of light(anti-)nuclei might serve as a baseline for understanding the debated nature of exotic states such as the X(3872), that has been interpreted as tetraquark state or hadronic molecule [?, ?].

2 Coalescence approach

2.1 Simple coalescence

In simple coalescence, nucleons produced in the collision coalesce into nuclei if they are close in space and have similar velocities [?, ?]. For a nucleus with mass number $A = Z + N$, the coalescence probability is typically quantified in terms of the coalescence parameter B_A, which is defined as

$$E_A \frac{\mathrm{d}^3 N_A}{\mathrm{d}p_A^3} = B_A \left(E_\mathrm{p} \frac{\mathrm{d}^3 N_\mathrm{p}}{\mathrm{d}p_\mathrm{p}^3} \right)^Z \left(E_\mathrm{n} \frac{\mathrm{d}^3 N_\mathrm{n}}{\mathrm{d}p_\mathrm{n}^3} \right)^N \Bigg|_{\vec{p}_\mathrm{p}=\vec{p}_\mathrm{n}=\frac{\vec{p}_A}{A}} , \tag{1}$$

where $p_{\mathrm{p,n}}$ are the momenta of the proton and neutron and $E_{p,n}$ their energy. Since at LHC energies the number of produced protons and neutrons at midrapidity is expected to be equal, the equation simplifies to

$$E_A \frac{\mathrm{d}^3 N_A}{\mathrm{d}p_A^3} = B_A \left(E_\mathrm{p} \frac{\mathrm{d}^3 N_\mathrm{p}}{\mathrm{d}p_\mathrm{p}^3} \right)^A \Bigg|_{\vec{p}_\mathrm{p}=\frac{\vec{p}_A}{A}} \tag{2}$$

Moreover, the LHC is particularly suited for the production of anti-nuclei, since the number of baryons and anti-baryons is essentially equal at midrapidity [?]. In a simple coalescence approach, the coalescence parameter is expected to be independent of p_T and of the object size with respect to the volume of particle emission (hereafter referred to as "source volume" or "source size"). In this naive expectation, the number of nuclei produced by coalescence increases with increasing number of nucleons produced in the collision. If the nucleon number increases with the event multiplicity, so does the number of (anti-)nuclei. While this picture is found to be approximately valid in pp and p–Pb collisions [?, ?], it breaks down in Pb–Pb collisions, that exhibit a strong decrease of B_A with the centrality of the collision [?]. In addition, the elliptic flow of deuteron cannot be explained by simple coalescence [?].

2.2 Full coalescence

In contrast to the simple approach described in the previous section, a more advanced coalescence model takes into account the size of the particle emission source, as the coalescence probability naturally decreases for two nucleons with similar momenta that are produced far apart in configuration space. While there are several approaches to address this effect [?], we rely in our study on the formalism

Mass number	Nucleus	Composition	B_E (MeV)	rms radius of wavefunction (fm)	Refs.
A = 2	d	pn	2.2	3.2	
A = 3	^{3}H	pnn			
	^{3}He	ppn			
	$^3_\Lambda$H	pΛn			
A = 4	^{4}He	ppnn			
	$^4_\Lambda$H	pΛnn			
	$^4_{\Lambda\Lambda}$H	p$\Lambda\Lambda$n			
	$^4_\Lambda$He	ppΛn			

Table 1: Properties of nuclei and hyper-nuclei. B_E is the binding energy per nucleon in MeV and the radius is given in terms of the rms radius of the wavefunction. References are given in the last column.

proposed in [?]. Consider mentioning the approximations done by Uli in his paper, if there is time and how Uli's paper relates to the Wigner formalism. In this approach, the quantum mechanical nature of the coalescence products is explicitly accounted for by means of an average quantum mechanical correction factor, $\langle C_A \rangle$. In the case of the deuteron, the quantum mechanical correction factor $\langle C_d \rangle$ has been approximated as

$$\langle C_d \rangle \approx \frac{1}{\left[1 + \left(\frac{r_d}{2R_\perp(m_T)}\right)^2\right] \sqrt{1 + \left(\frac{r_d}{2R_\parallel(m_T)}\right)^2}} \tag{3}$$

where r_d is the radius of the deuteron, $R_\perp$ and $R_\parallel$ are the lenghts of homogeneity of the coalescence volume and m_T is the transverse mass of the coalescing nucleons. The size of the nucleus enters in the determination of the coalescence parameter B_2 via the quantum-mechanical correction factor $\langle C_d \rangle$, as well as the homogeneity volume $R_\perp^2 R_\parallel$, according to the relation

$$B_2 = \frac{3\pi^{3/2}\langle C_d \rangle}{2m_T R_\perp^2(m_T) R_\parallel(m_T)} \tag{4}$$

which is the main result of [?]. It is interesting to note that the coalescence parameter decreases with increasing volume, as expected. In addition to this, the quantum mechanical correction factor introduces a length scale defined by the deuteron size relative to the source size in the calculation of B_2, which reflects the coalescence probability. If we assume that $R_\perp \approx R_\parallel \approx R$, Eqs. 3 and 4 simplify to

$$\langle C_d \rangle \approx \left[1 + \left(\frac{r_d}{2R(m_T)}\right)^2\right]^{-3/2} \tag{5}$$

and

$$B_2 = \frac{3\pi^{3/2}\langle C_d \rangle}{2m_T R^3(m_T)}. \tag{6}$$

Figure 1 shows the source radius (R) dependence of the quantum-mechanical correction factor (on the left) and the coalescence parameter B_2(on the right), calculated assuming (a.) a point-like nucleus, (b.) $r_d = 0.3$ fm as currently assumed in thermal model calculations [?], (c.) the current estimate of the rms radius of the deuteron $r_d = 3.2$ fm [?], (d.) a larger, irrealistic value of $r_d = 10$ fm.

- describe qualitatively what is visible in the figure that heavy-ion collisions are similar while production of "large" objects is suppressed in small collsion systmes

Following the approach and discussion presented in [?], Eq. 3 may be generalised as

$$\langle C_A \rangle = \prod_{i=1,2,3} \left(1 + \frac{r^2}{4R_i^2}\right)^{-\frac{1}{2}(A-1)} \tag{7}$$

for mass number A and the radii R_i which describe the volume of the emitting source.

- add formula from Kfir for B3 and write how it relates to Uli's (or it is derived from it)

2.3 Source volume

- describe what ALICE actually measures for multiplicity and say it is known that system size increases with multiplicity (linearly or approx.)

- assumption 1: parameterisation we propose, which is found to describe the deuteron data

- plot our parameterisation vs the HBT results

- excess binding energy needs to be released to the system to make coalescence work

3 Statistical-thermal approach and blast-wave

-

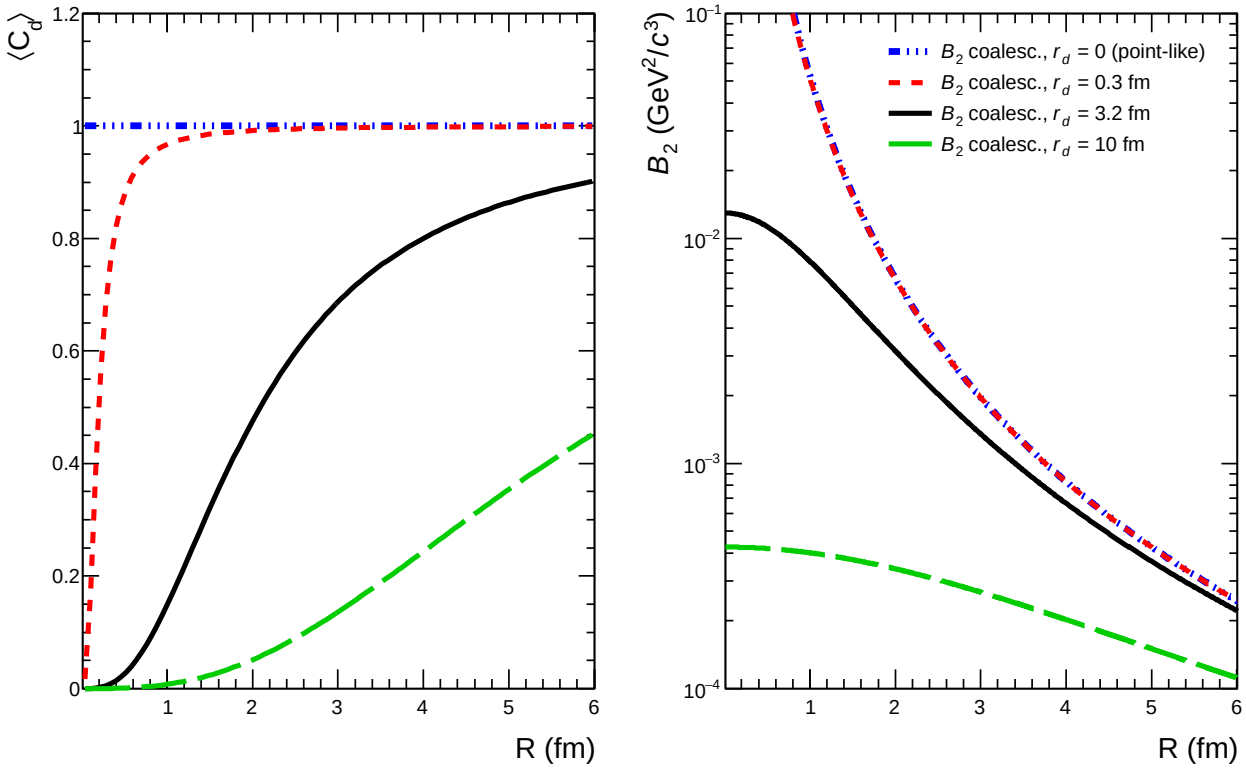

Figure 1: The quantum mechanical correction factor $\langle C_d \rangle$ (left panel, see Eq. 5) and the coalescence parameter B_2 for deuteron (righ panel, see Eq. 6) as a function of the radius of the source, R, calculated assuming a radius of the deuteron $r_d = 0, 0.3, 3.2$ and 10 fm.

Figure 2: Cd vs radius, B2 for point-like objects and realistic wavefunctions

Figure 3: Parameterisation of the dependence of the source radius on multiplicity assumed in this paper, compared to HBT data.

4 Comparison with experimental data

4.1 (Anti-)nuclei with $A = 2$, 3, 4

4.2 (Anti-)hyper-nuclei

5 Projections for the LHC Run 3 and 4

6 Summary and conclusions

We conclude that (c.) appears unlikely, thus leaving (b.) as a viable option, at least with our present knowledge of the hypertriton size.

Acknowledgements

The authors would like to thank themselves for the auto-critics.